

Evaluation on Interaction Surface of Plastic Resistance for Exposed-type Steel Column Bases under Biaxial Bending

Jae-hyook Choi*, Kenichi Ohi

*Department of Architecture and Civil Engineering, Kobe University,
1-1Rokodai-cho, Nada-ku, Kobe 657-8501, Japan*

Exposed-type steel column bases are used widely in low-rise building construction. Numerous researchers have examined methods to identify their stiffness and strength, but those studies have heretofore been restricted to in-plane behaviors. This paper presents an experimental investigation of inelastic behaviors of square hollow section (SHS) steel column bases under biaxial bending. Two types of failure modes are considered: anchor bolt yielding and base plate yielding. Different pinching effects and interaction surfaces for biaxial bending are observed for these two modes during bi-directional quasi-static cyclic loading tests. Differences are elucidated using limit analyses based on a simple analytical model.

Key Words: Interaction Surface, Biaxial Bending, Limit Analysis, Loading Path, Convex Set

1. Introduction

Considerable damage occurred to steel structures during the Hyogo-ken Nanbu Earthquake in Japan. Numerous exposed-type column bases failed in several consistent patterns caused by brittle base plate fracture, excessive anchor bolt elongation, unexpected early anchor bolt failure, and inferior construction work. An exposed-type column base receives axial force and biaxial bending when receiving an arbitrary multi-directional earthquake motion. For this reason, it is more desirable to consider effects of biaxial bending at the ultimate stage of inelastic response in the design of steel column bases.

This study experimentally examined inelastic behavior and the ultimate resistance of exposed-type steel column bases subjected to biaxial bending. Limit analysis of the exposed-type column

bases was conducted to further confirm the interaction surface, which is correlated to resistance strength of the bi-directional load in a column base. As mentioned above, buildings are invariably subjected to cyclic biaxial lateral load with varying axial load (compressive and tensile load) during earthquakes: the column bases and the behavior of column bases change dramatically according to axial load changes. Thus, as a first step to evaluate the behavior of column bases under arbitrary seismic excitation, we are concerned with the correlates of resistance strength for the lateral bi-directional load, which are x -axis and y -axis bending in the column bases. No axial load is applied to the column bases.

2. Outline of Experimental Program

These studies are conducted on exposed-type steel column bases comprising a square hollow section (SHS) steel column, two types of base plates of 9 mm and 19 mm thickness, anchor bolts (fully threaded) and a base block. Systems comprising those elements are set up as a cantilever column. Then each test specimen is subjected to a different lateral displacement history. The test setup and the test specimen dimensions are shown

* Corresponding Author,

E-mail: jhchoi@kobe-u.ac.jp

TEL: +81-90-3526-4556; FAX: +81-78-803-6048

Department of Architecture and Civil Engineering,
Kobe University, 1-1Rokodai-cho, Nada-ku, Kobe
657-8501, Japan. (Manuscript Received September 6,
2004; Revised January 25, 2005)

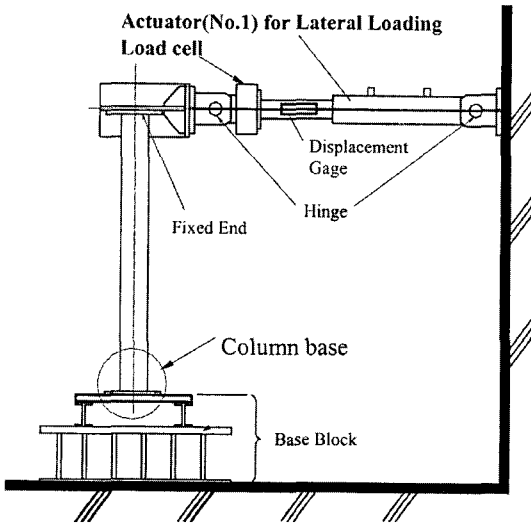


Fig. 1 Test setup

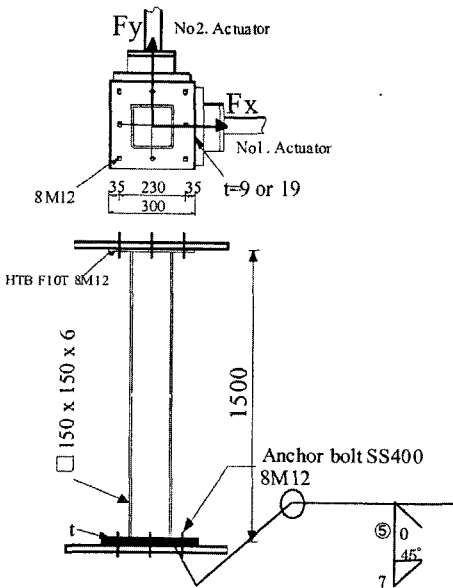


Fig. 2 Dimensions of specimen

respectively in Fig. 1 and Fig. 2. Experiments are conducted in two uniaxial series of and four biaxial series of quasi-static cyclic loading tests on cold-formed \square -150×150×6 columns connected by a semi-rigid column base to a rigid foundation. Table 1 gives details of the test code.

2.1 Loading programs

During quasi-static cyclic loading tests under biaxial bending, the column is subjected to a la-

Table 1 Tests code

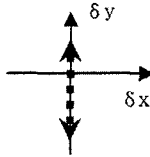
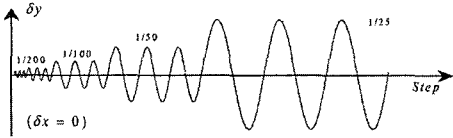
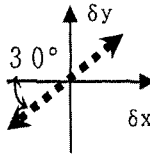
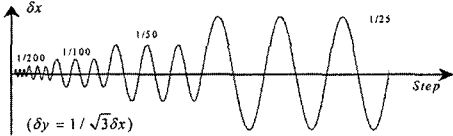
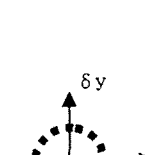
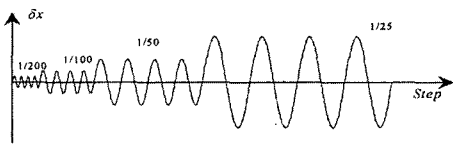
Loading type	Uniaxial Y (UY)	Biaxial-Linear (BL)	Biaxial-Circular (BC)
19 mm	ECB19SCUY	ECB19SCBL	ECB19SCBC
9 mm	ECB9SCUY	ECB9SCBL	ECB9SCBC

Note: ECB stands for 'Exposed-type Column Base' and SC stands for 'quasi-Static Cyclic'

t: Thickness of base plate

teral force on each loading direction. The experiment is conducted in six series of tests: first, uniaxial quasi-static cyclic loading is done in the y-direction (SCUY), then biaxial linear quasi-static cyclic loading (SCBL), and finally biaxial circular quasi-static cyclic loading (SCBC) for 9 mm and 19 mm thick column bases. Table 2 shows loading program details. Only displacement control is adopted to ensure an accurate loading path in the x-y plane. Because of the perpendicular arrangement of two actuators (Fig. 3), the movement of one actuator changes the other actuator's direction. The change in the actuator's direction is evaluated and compensated by a computer to overcome that problem. At the beginning of testing, the target amplitude of δ/L ratio, which is the drift angle, is taken as 1/200, where L denotes the effective length of column and δ denotes the displacement at the top of the column. After completion of every three loading cycles, the displacement amplitude is increased sequentially to 1/100, 1/50, and 1/25 (in case of SCBC is every four loading cycles). For every test, loading is done quasi-statically, slower than 0.001 m/s at the loading velocity. In uniaxial quasi-static cyclic loading in y-direction (SCUY), the load is applied uniaxially only in the y-direction; no loading is done in the x-direction. In biaxial linear quasi-static cyclic loading (SCBL), the ratio of $\delta y/\delta x$ is taken as $1/\sqrt{3}$, which means that the loading direction makes an angle of 30° with the y-axis. In biaxial circular quasi-cyclic loading (SCBC), deflection in the perpendicular direction also starts after 0.75 cycles in the direction of the x-axis. Loading is applied by displacement in the y-axis direction. Then, the test specimen is rotated three times around its vertical

Table 2 Loading Program

Loading Type	Displacement path	Control program for top displacement
SC-UY	 <p>Uniaxial-Y</p>	 <p>($\delta x = 0$)</p>
SC-BL	 <p>Biaxial-Linear</p>	 <p>($\delta y = 1/\sqrt{3}\delta x$)</p>
SC-BC	 <p>Biaxial-Circular</p>	

* δ : column top displacement

axis. After completion of 3.75 cycles, it returns to its starting point because of the loading applied in the x -axis direction.

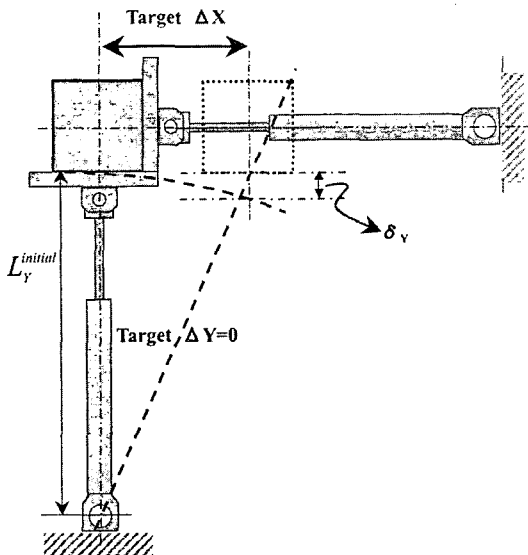


Fig. 3 Geometric error correction in biaxial testing

2.2 Material properties

Material properties for the 19 mm and 9 mm thick base plates were determined from tensile coupon tests on strip cuts taken from a part of the steel base plates. Furthermore, for the anchor bolts, ten pieces were chosen randomly, and tested. The yield stress σ_y and the tensile strength σ_u

Table 3 Material properties (MPa)

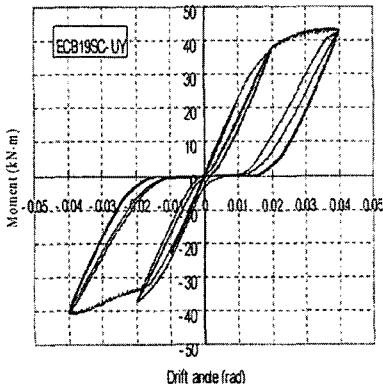
	σ_y	σ_u
Base plate 9 mm (JIS SS400)	270	450
Base plate 19 mm (JIS SS400)	250	430
SHS 150×150×6 (JIS STKR 400)	782	902
	(kN)	
	T_y	T_u
M12 A. bolt (JIS SS400) (all threaded)	53	57

of base plates (with 9 mm, 19 mm thickness) and square hollow section steel column, and the tension load capacity T_y , T_u of anchor bolt are summarized in Table 3.

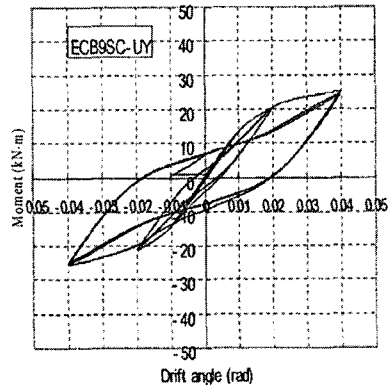
2.3 Test results

2.3.1 Hysteretic responses

Hysteretic responses of the test specimen are

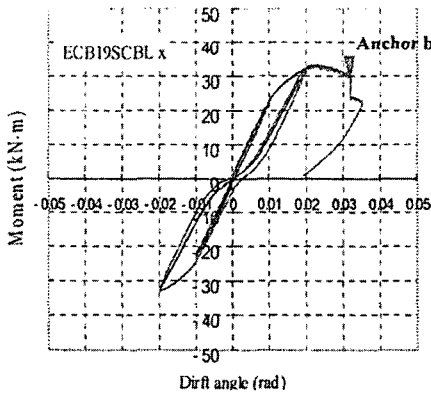


(a) ECB19SCUY

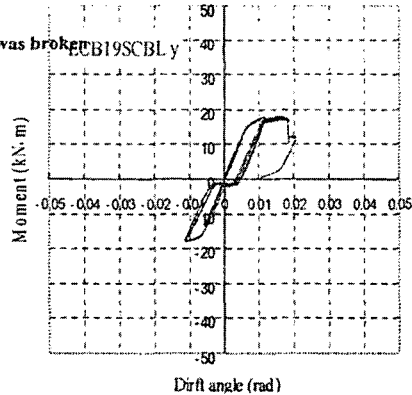


(b) ECB9SCUY

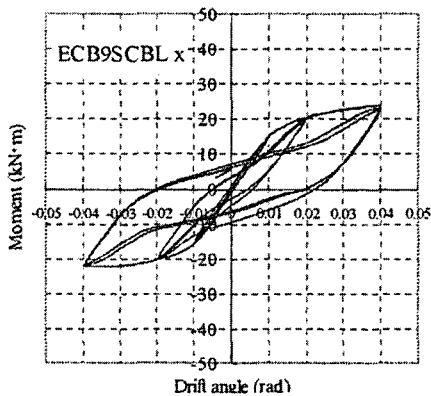
Fig. 4 Hysteretic loops for SCUY



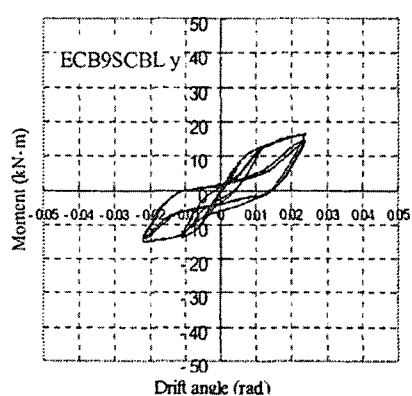
(a) ECB19SCBL-x



(b) ECB19SCBL-y



(a) ECB9SCBL-x



(b) ECB9SCBL-y

Fig. 5 Hysteretic loops for SCBL

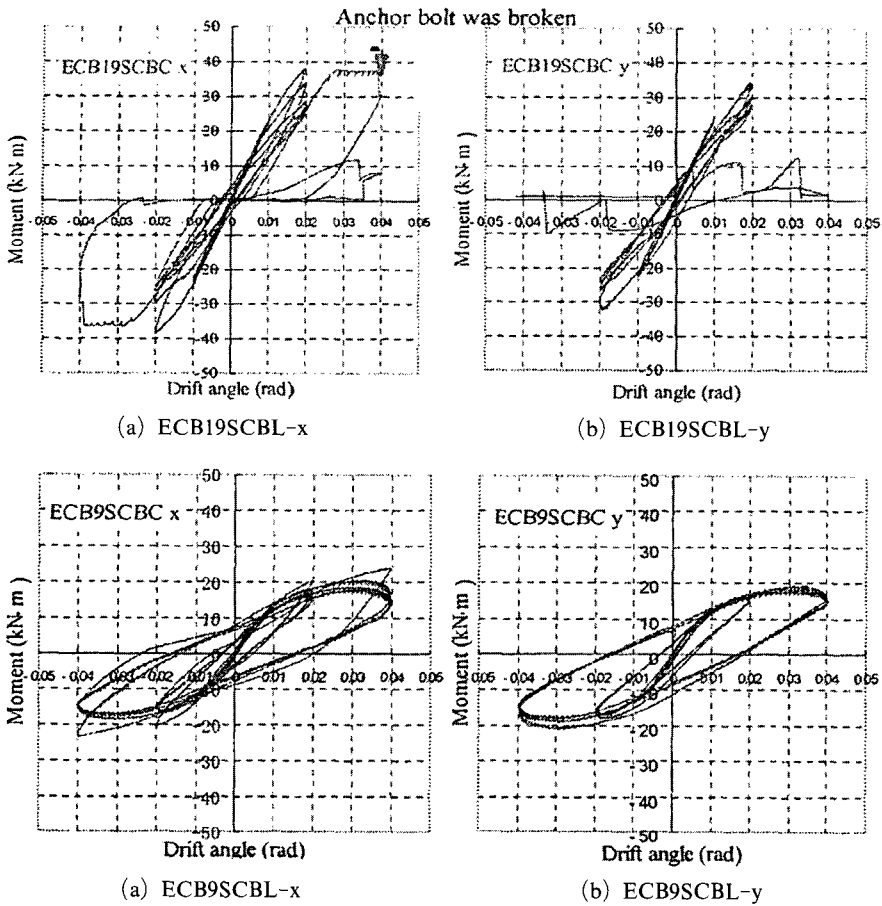


Fig. 6 Hysteresis loops for SCBC

shown in Figs. 4~6. During tests, the SHS column remained in elastic range.

In the test series of the 19 mm base plate, the anchor bolt yielding mechanism was observed during cyclic loading. In all directions, the case of anchor bolt yielding showed pinched hysteretic behavior. Uniaxial loading failure of anchor bolt did not occur, but in the case of biaxial loading, ECB19SCBL and ECB19SCBC, an anchor bolt was broken when the drift angle on x -component passed 0.03 rad. On the other hand, in the 9 mm base plate test series, the base plate yielding mechanism was observed during cyclic loading tests. For the base plate, yielding type showed a less pinched, but slight degradation of hysteretic behavior. We have bi-linear characteristics in the first cycle of each three-cycle group, but the stiffness increases and pinched loops are observed at

the 2nd and 3rd cycle of each cycle group. Additionally, we observed that hysteretic behavior for the biaxial circular (ECB9SCBC) became more rounded at the unloading point.

2.3.2 Loci of biaxial bending

Loci of biaxial bending for ECB19SCBC and ECB9SCBC are shown in Fig. 7. It is noteworthy that the shapes of the interaction surfaces for the anchor bolt yielding type and the base plate yielding type differ for biaxial circular loading. The interaction surface shape of anchor bolt yielding maintains an almost circular shape until the anchor bolt is broken. In contrast, the shape of the interaction surface of the base plate yielding type is circular in the elastic range; it changes to a square shape with rounded corners in the inelastic range.

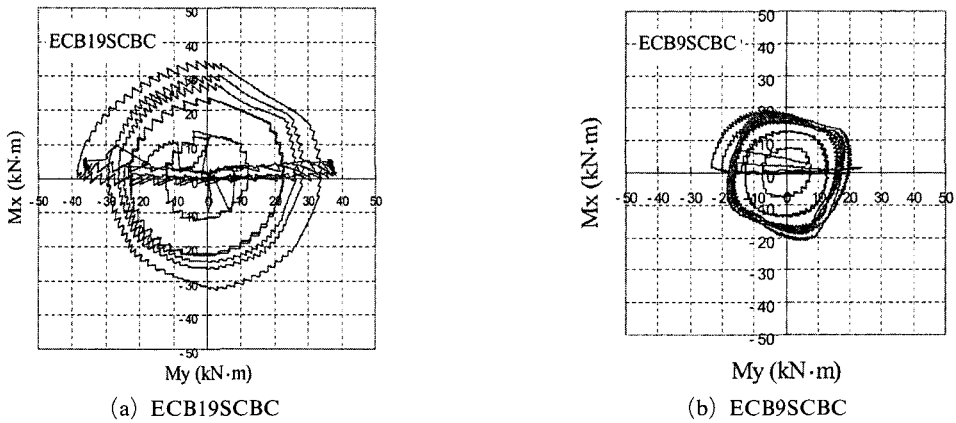


Fig. 7 Loci of biaxial bending moments

3. Analytical Model for Limit Analysis

We propose two different multi-spring models to examine interaction between x -axis and y -axis bending in a column base: anchor bolt yielding and base plate yielding models.

3.1 Analytical model of anchor bolt yielding type

Figure 8 shows that the column base is modeled with an analytical model in which the anchor bolts yield, but the base plate does not yield. The base plate is assumed to rotate around compression springs beneath the column flange because part of the column flange is applied to compression force. This compression does not operate against tension force. On the other hand, the tension spring that is not operating against compression force is set on the anchor bolt. Fig. 9 shows that the equilibrium equation can be derived considering only the tension and compression spring forces.

3.1.1 Compact procedure

The following problem is solved through limit analysis based on linear programming (Compact Procedure, (Liversley, 1976)):

$$\text{Maximize } \lambda \tag{1}$$

Subject to:

$$\text{Equilibrium equation } \lambda \{P\} = [Con] \cdot \{m\} \tag{2}$$

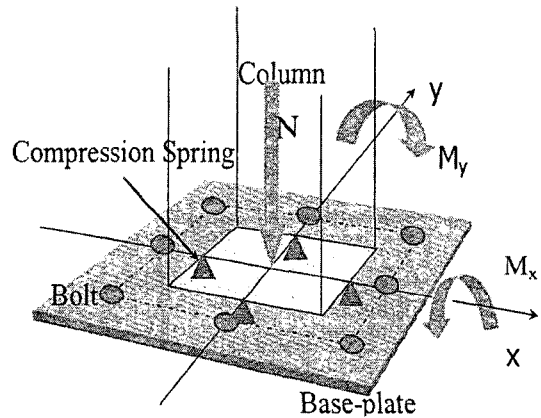


Fig. 8 Analytical model of anchor bolt yielding

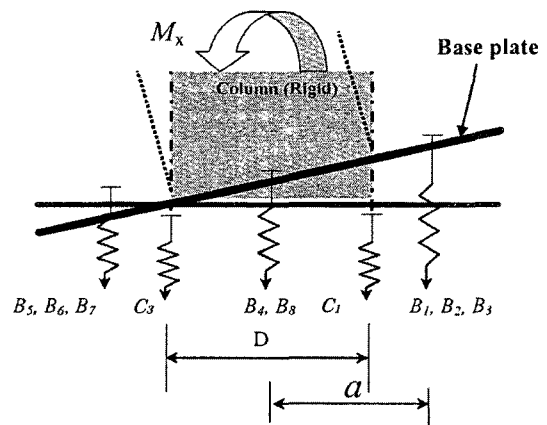


Fig. 9 Equilibrium between axial-spring and generalized stress in y -axis

$$\text{Plastic condition } |m_i| \leq m_{pi} \tag{3}$$

where λ is a load factor, $\{P\}$ is the load pattern vector, $[Con]$ is the connectivity matrix, $\{m\}$ is element force vector, m_i is component of $\{m\}$ and m_{pi} is plastic capacity of the i -th element. The equilibrium equation of the model in Fig. 9, which gives a relationship between the load and element force, is as follows :

$$\begin{Bmatrix} M_x \\ M_y \\ N \end{Bmatrix} = \begin{bmatrix} a & a & a & 0 & -a & -a & -a & 0 & -\frac{D}{2} & 0 & \frac{D}{2} & 0 \\ -a & 0 & a & a & a & 0 & -a & -a & 0 & -\frac{D}{2} & 0 & \frac{D}{2} \\ 1 & 1 & 1 & 1 & 1 & 1 & 1 & 1 & 1 & 1 & 1 & 1 \end{bmatrix} \begin{Bmatrix} B_1 \\ B_2 \\ B_3 \\ B_4 \\ B_5 \\ B_6 \\ B_7 \\ B_8 \\ C_1 \\ C_2 \\ C_3 \\ C_4 \end{Bmatrix} \quad (4)$$

The plastic condition of this model is as follows
 anchor bolt, $0 \leq B_i \leq B_{ui}$
 compression spring, $-C_{ui} \leq C_i \leq 0$ (5)

Therein, B_{ui} and C_{ui} represent the respective ultimate strengths of anchor bolts and the concrete basement. Additionally, $C_{ui} = \infty$ that is, the concrete foundation does not fail.

3.1.2 Linear mapping of extreme points in s convex set (Ohi, 2001)

A set in Euclidean space E^m is a convex set if it contains all line segments connecting any pair of its points.

The fundamental concepts of convex set theory are as follows (Fig. 10):

- (1) Each point in a convex set is expressed using an extreme point ;
- (2) A set T in an Euclidean space E^m formed by linear-mapping from convex set S in E^n space becomes a convex set ;
- (3) Extreme points of convex set T exist in images of the extreme points in convex set S .

First, the equilibrium equation between generalized stress (axial force and biaxial bending) and the axial force of nth axial-spring is set up to

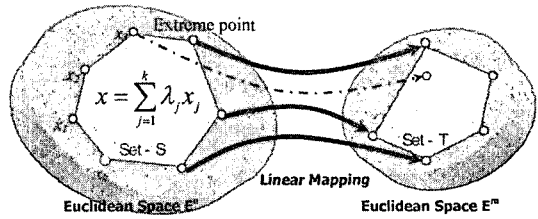


Fig. 10 Convex set theory

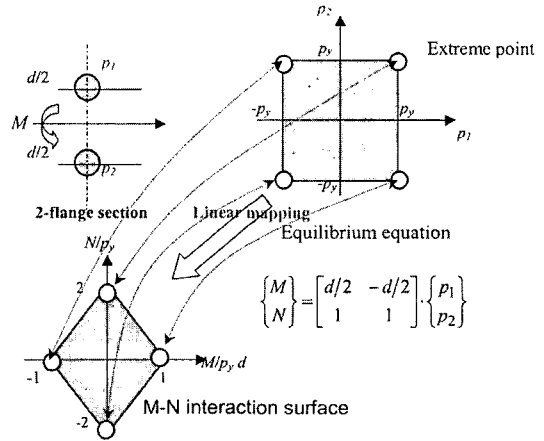


Fig. 11 Interaction surface of a two-flange section

capture the generalized stress space that satisfies the conditions of equilibrium and plasticity.

$$\begin{Bmatrix} M_x \\ M_y \\ N \end{Bmatrix} = \begin{bmatrix} C_{spring} \end{bmatrix} \begin{Bmatrix} p_1 \\ p_2 \\ \vdots \\ p_n \end{Bmatrix} \quad (6)$$

For the n -dimension space of axial-spring force, the domain, which satisfies the plastic condition for each axial spring, becomes an n -dimensional polyhedron. This n -dimensional polyhedron is a convex set with 2^n extreme points.

$$\{p^*\} = \{\pm p_{y1}, \pm p_{y2}, \dots, \pm p_{yn}\}^T \quad (7)$$

The interaction surface of two-flange section is shown in Fig. 11 based on convex set theory. It is possible to obtain an accurate M - N interaction surface through linear mapping of extreme points in each axial spring plastic condition.

3.2 Analysis model of base plate yielding type

Figure 12 shows that the column base is modeled with an analytical model in which the anc-

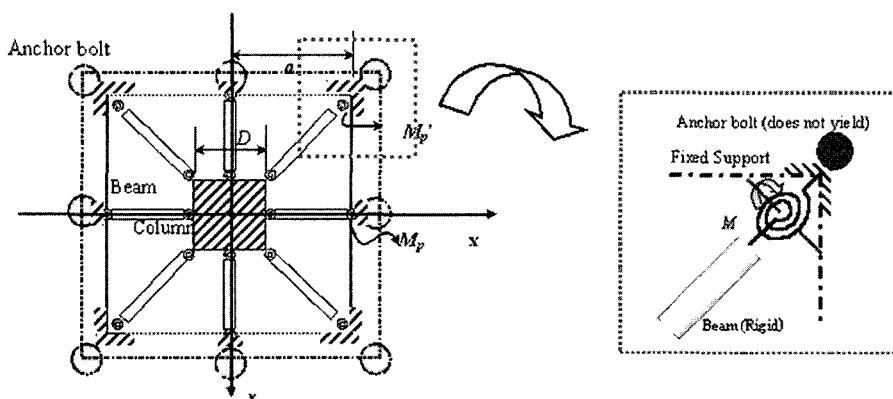


Fig. 12 Analytical models of base plate yielding

hor bolts do not yield, but the base plate yields. Fig. A shows that the base plate is approximated as eight beams with a certain effective width.

3.2.1 In the case of uniaxial bending

The ultimate strength is given by the following equation based on the virtual-work principle when bending is applied uniaxially.

$$\begin{aligned} M_{xp} = M_{yp} &= \sqrt{2} \frac{2+2\gamma}{1-\gamma} Mp' + \frac{1+7\gamma}{1-\gamma} Mp \\ &= \frac{\sqrt{2} \xi (2+2\gamma) + 1+7\gamma}{1-\gamma} Mp \end{aligned} \quad (8)$$

Therein, Mp and Mp' are the respective full-plastic moments for effective widths b_{eff} and b_{eff}' . The ratio of the effective width of base plate near the column corner to that of the base plate near the column side (Appendix A) is ξ . The ratio of the lengths $D/2$ to a is γ .

3.2.2 In the case of biaxial bending (45°)

The ultimate strength in the direction making a 45° angle with x and y -axis is greatest when biaxial bending is applied. The ultimate strength in the direction making a 45° angle with both axes is given by the following :

$$\begin{aligned} M_{45p} &= 2 \frac{1+3\gamma}{1-\gamma} Mp' + 2 \frac{3\sqrt{2}\gamma}{1-\gamma} Mp \\ &= 2 \frac{\xi(1+3\gamma) + 3\sqrt{2}\gamma}{1-\gamma} Mp \end{aligned} \quad (9)$$

4. Comparisons with Test Results

Actually, the resistance interaction surface for the steel column bases experiences movement, expansion and rotation according to the applied load history. For that reason, it is difficult to evaluate it as just one case of a biaxial circular-loading test. Therefore, this paper presents results for the resistance interaction surface derived from the uniaxial, biaxial linear (30°) and biaxial circular loading tests. Especially because of specimen symmetry, it is possible to regard biaxial linear loading test results as those for loading in 12 directions. Consequently, the shape of the resistance interaction surface can be derived.

4.1 Interaction surface on anchor bolt yielding type

The analysis result of an anchor bolt yielding type under biaxial bending is shown in Fig. 13 (a). Here, the ultimate strength of the anchor bolt is $B_u = 57$ kN ; the ratio of length is $\gamma = 0.65$ ($a = 115$ mm).

Although the resistance force of biaxial circular loading test results gradually degraded, the interaction surface on the anchor bolt yielding type approximately agrees with the analysis result. Results of uniaxial and biaxial linear tests concur with the analysis result. For the reasons mentioned above, the shape of the interaction surface on the anchor bolt yielding using the thick base

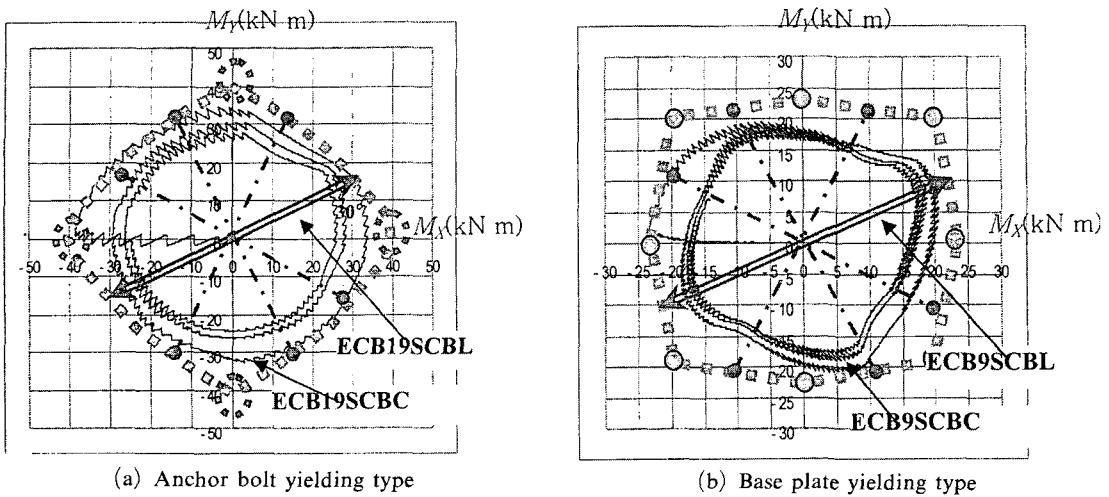


Fig. 13 Comparison of results

plate is a circle or diamond shape.

4.2 Interaction surface on base plate yielding type

The analysis result of base plate yielding type under biaxial bending is shown in Fig. 13(b). A safety domain under biaxial bending of the base plate yielding type is obtained by calculating the resistance forces in both uniaxial direction and in directions deviating 45° from the x - and y -axes. The following theorem can be used to estimate the safety domain: The safety domain is a convex set. A convex combination of two arbitrary points in a convex set that is a line-segment between two points is a part of the convex set. Here, the effective width to calculate the moment capacity of the base plate is estimated after (Appendix). The moment capacity of base plate is $M_p = 0.87$ kN m, where ($b_{eff} = 92$ mm, $\sigma_u = 450$ MPa). The ratio of length is $\gamma = 0.65$; the ratio of effective width is $\zeta = 0.8$.

At the end of the first cycle, at the initiation of circular movement, the analyzed strength matches with the test resistance. However, in subsequent reversals, the test resistance diminishes as shown in Fig. 13(b). The probable reason is that some small welding cracks appear during loading path between the column corner and the base plate. Some deterioration of resistance is observed. However, the shape of the analyzed interaction

surface of base plate yielding using the thin base plate is a square and closely resembles the test result.

5. Conclusions

A series of quasi-static cyclic loading test on the exposed-type steel column bases under biaxial bending was carried out. To confirm the interaction surface of the bi-directional load in a column base, limit analysis was performed on the exposed-type column bases. The conclusions drawn from this study are as follows:

(1) Anchor bolt yielding using a thick base plate showed pinched hysteretic behavior in all directions. On the other hand, base plate yielding using a thin base plate showed a less pinched, but slightly degraded, hysteresis behavior. Especially, the hysteretic loop for base plate yielding type began to show pinching from the second cycle of the each drift angle.

(2) The biaxial interaction surface shape differs for anchor bolt yielding and base plate yielding during biaxial circular loading. Anchor bolt yielding maintains an almost circular shape until the anchor bolts fail. On the other hand, base plate yielding shows a circular shape in the elastic range and changes to a square shape with rounded corners in the inelastic range.

(3) Biaxial interaction surfaces of limit analysis for the anchor bolt yielding model and base plate yielding model approximately agree with the test results. Limit analysis explains the different interaction surfaces of the anchor bolt yielding type and the base plate yielding type. These tests and analyses examined only the standard case, in which eight anchor bolts are arranged symmetrically. The shapes of the interaction surface of an exposed-type steel column base may be influenced by the anchor bolt arrangement when biaxial bending is applied. Respective cases must be analyzed when they differ from the standard arrangement treated here.

References

AIJ, 1998, Recommendation for Limit State Design of Steel Structures.

Bousias, S. N., 1995, "Load Effects in Column Biaxial Bending with Axial Force," *Journal of Engineering Mechanics*, Vol. 121, No. 5, pp. 598~605.

Choi, J. H., Ohi, K., Shimawaki, Y., Oktem, C. and Ito, T. 2003, "Experimental Study of Inelastic Behavior of Exposed-type Steel Column Bases Under Biaxial Bending," *Bulletin of Earthquake Resistant Structure Research Center, Institute of Industrial Science, University of Tokyo*, No. 36, May.

Choi, J. H., Ohi, K., Oktem, C., Shimawaki, Y. and Ito, T., 2003, "Inelastic Behavior of Exposed-type Steel Column Bases under Biaxial bending (Part 2 : Results of Biaxial Cyclic Loading Tests)," *Proc. Of Architectural Research Meetings*, Kanto Chapter, AIJ.

Choi, J. H. and Ohi, K., 2004, "Dynamic Characteristic Identification on Steel Column bases Installed in Pendulum-type Earthquake Response Observatory," *KSME International Journal*, Vol. 18, pp. 2225~2235

Kadoya, H., Watanabe, T., Suzuki, M., Hagino, T. and Someya, T., 1998, "Experimental Study on Mechanical Characteristics of Steel Tubular Column Bases," *Journal of Constructional Steel*,

Vol. 6, pp. 261~268.

Liversley, R. K., 1976, "Matrix Method of Structural Analysis (2nd ed.)," Pergamon Press.

Ohi, K., 1993, *Limit Analysis : Lecture Note for Training Course in Seismology and Earthquake Engineering of IISEE*, JICA, Tsukuba.

Ohi, K., Sun, H. and Ito, T., 2001, "Matrix Method of Limit Analysis on Framed Structures Considering Interacted Bending and Axial Resistances," *J. Struct. Constr. Eng.*, AIJ, No. 539, pp. 71~77.

Ohi, K., Tanaka, H. and Takanashi, K., 1981, "Ultimate Strength of Steel Column Bases," *J. Struct. Constr. Eng.*, AIJ, No. 308, pp. 14~23.

Watanabe, E., Sugiura, K. and Oyawa, W. O. 2002, "Effect of Multi-Directional Displacement Path on the Cyclic Behaviour of Rectangular Hollow Steel Columns," *Structural Eng./Earthquake*, JSCE, Vol. 17, No. 1, pp. 69s~85s.

Appendix A

Moment resisting capacity of base plate (Kodaka et al., 1998).

Effective width of the base plate resisting to the bending moment is estimated. First, the effective angle at the corner of base plate shown in Fig. A is estimated. The effective length is calculated. The effective angle at the corner of base plate is estimated as 60°.

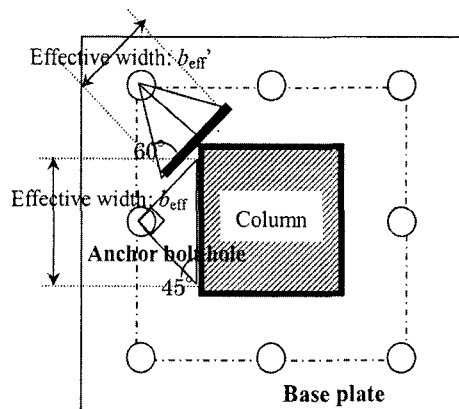


Fig. A Effective width at the base plate corner